Study of the Miscibility and Mechanical Properties of NBR/HNBR Blends

IBNELWALEED A. HUSSEIN*, REHAN A. CHAUDHRY, *and* BASEL F. ABU SHARKH

Department of Chemical Engineering
King Fahd University of Petroleum & Minerals
Dhahran 31261, Saudi Arabia

In this study, hydrogenated acrylonitrile butadiene rubber (HNBR, ZETPOL-2010L) and nitrile butadiene rubber (NBR, NIPOL-DN4555) were blended at different ratios in a Haake melt blender at 130°C. The HNBR and the NBR were of very similar acrylonitrile content and Mooney viscosity. The melt miscibility and solid-state properties were investigated by rheological, thermal, and mechanical testing and scanning electron microscopy (SEM) techniques. The dynamic viscosity of the blends followed the log-additivity rule, while the flow activation energy closely followed the inverse additivity rule. On the other hand, the storage modulus showed synergistic effects at all compositions, suggesting the presence of emulsion morphology at both ends of the composition range. For the 50/50 HNBR/NBR blend, the SEM micrographs suggest a uniform elongated structure. The thermal analysis showed the presence of two glass transitions, representing the pure components, at all blend ratios, suggesting the absence of segmental miscibility of the blends. The small-strain mechanical properties such as tensile modulus and yield stress followed linear additivity. However, HNBR and HNBR-rich blends were observed to strain harden at a rate higher than that of NBR. Induced crystallization of HNBR was suggested to be the reason for the strain hardening. The different rheological, thermal, and mechanical testing techniques agree in suggesting that the structurally similar HNBR and NBR are not thermodynamically miscible but mechanically compatible.
Polym. Eng. Sci. 44:2346–2352, 2004. © 2004 Society of Plastics Engineers.

INTRODUCTION

Nitrile butadiene rubbers (NBRs) belong to the class of specialty elastomers that offer a broad range of thermal and oil resistance properties. These elastomers are extensively used in automobile and oil-drilling applications (1). Continuous performance demand by these industries led to the development of hydrogenated nitrile butadiene rubber (HNBR). Removal of double bond in the backbone of the polymer by catalytic hydrogenation results in improved UV and ozone resistance. The two main methods for this catalytic reaction are homogenous and heterogeneous catalytic reactions (2). Most of the previous literature suggests that homogenous catalytic reactions were preferred over heterogeneous ones. However, the major weakness of homogenous catalytic hydrogenation reactions is the difficulty in removal of the catalyst from the polymer mixture, and this is in fact the main reason for the high cost of HNBR (3).

Blending of rubbers is an important route for developing new polymeric materials with tailored physical properties. Blends of butadiene rubbers and other polymers have received wide attention in the literature during the last two decades (4–19). The role of NBR as a compatibilizer has also been investigated (5). Processing conditions—such as mixing speed, blending time, and temperature—were reported to have a strong influence on the ultimate properties of the blend (6, 8, 15). Also, blend morphology and compatibility were found to be affected by structural parameters such as acrylonitrile (ACN) content and Mooney viscosity (6, 16). These molecular parameters, characteristic of nitrile elastomers, influence blend miscibility as well as the size of dispersed phase (6). Nitrile rubbers are considered to be polar rubbers (17).

Severe and White studied the miscibility of HNBRs with chlorinated polymers and found that strong interactions

*To whom correspondence should be addressed.
E-mail: ihussein@kfupm.edu.sa
© 2004 Society of Plastics Engineers
Published online in Wiley InterScience (www.interscience.wiley.com).
DOI: 10.1002/pen.20263

between the functional groups are responsible for miscibility (18). HNBR was suggested to be immiscible with polyisoprene and SBR and miscible with chlorinated polyethylene. Blends compatibility of NBR and other elastomers such as natural rubber (NR) (6, 15) and polystyrene-co-acrylonitrile (16) were studied.

As mentioned earlier, the difficulty of removing the catalyst from HNBR is the main cause of its high price. Blending of unsaturated NBR and the more flexible HNBR molecules has its economic and scientific reasons. The resulting product may offer a relatively cheap alternate in the same applications where these are used in pure form. Available studies indicate that NBR and HNBR have been extensively studied for their blends with other plastics and elastomers. Interestingly, not many studies were reported in the public literature on the blends of NBR and HNBR elastomers.

In the present study, the blend miscibility of NBR and HNBR was studied in the complete composition range. A study of the melt miscibility and its implications on the solid-state properties is performed using rheological, thermal analysis, mechanical testing, and scanning electron microscopy (SEM) techniques. This study mainly highlights the compatibility of NBR/HNBR blends.

Blend morphology is also known to be an indicator of blend compatibility (6, 10, 15, 18). Generally, a smaller phase size of the dispersed phase results in better blend compatibility, and improved properties (6, 15, 17). For immiscible systems, the state of dispersion and the shape of the dispersed phase greatly influence the rheological responses. Emulsion morphology causes the storage modulus, G′ and loss modulus, G″, to exceed values for the more viscous component. Scholz *et al.* derived a constitutive equation for dilute emulsions of such nature. The two liquids are assumed to be incompressible and totally immiscible (19, 20). The emulsion was shown to haves dynamic moduli given by

$$G'(\omega) = \frac{\eta_m^2 \phi}{80(\alpha/R)} \left(\frac{19k + 16}{k + 1} \right)^2 \omega^2 \qquad (1)$$

where η_m is the viscosity of the matrix liquid; $k = \eta_d / \eta_m$ where η_d is the viscosity of the dispersed droplets; R is the radius of the dispersed domains; α is the surface tension between the two liquids; and is ϕ the volume fraction of the dispersed phase. In thermal analysis, a single T_g is a proof of segmental mixing of polymer molecules, and hence, blend compatibility (21).

EXPERIMENTAL

Materials

The NBR and HNBR samples used in this study were commercial samples obtained from Zeon Chemicals, USA. The NBR (NIPOL-DN4555) has an ACN content of 45%, specific gravity of 1, and a Mooney Viscosity of 48−63. On the other hand, the HNBR (ZETPOL-2010L) has an ACN content of 36, specific gravity of 0.95, a Mooney Viscosity of 50%−65%, and a 96% degree of hydrogenation. The two polymers represent the best Zeon NBR and HNBR products that closely match the ACN content and Mooney viscosity (ML_{1+4} at 100°C) with the degree of hydrogenation as the major difference. Also, the high ACN content NBR was found easy to handle in the rheological tests, compared to other low ACN–content brands. Similarly, the HNBR selected for this study had a high level of hydrogenation. The range of Mooney viscosities of the NBR and HNBR was close enough to reduce the effects of the viscosity ratio on blend miscibility (22).

Characterization

The elastomers were cut into small pieces and ground in a Fritsch grinding mill. Pure samples and blends of 10%, 30%, 50%, 70%, and 90% HNBR (w/w) were conditioned in a Haake Polydrive blender with Cam-type internal rotors. Conditioning was carried out at 130°C for 10 minutes and at 50 rpm. Owing to the high viscosity of the elastomers, the viscous heating effects were prominent, and in most of the cases the melt temperature was ~144°C. Earlier studies of degradation of these elastomers showed that the NBR and HNBR rubbers were stable at this temperature (23). The agreement of the rheology and light scattering of as-received and conditioned samples suggests no degradation of NBR and HNBR during the conditioning process (23). Air-cooled samples were molded in a Carver press at 150°C. Molding was conducted after preheating for 6 minutes. The loaded sample was then placed under 3 tons of pressure for 4 minutes, followed by an increase to 7 tons for 3 minutes. Then the mold was water-cooled for 10 minutes. The thermal and mechanical history in the press was the same for all samples. Samples from the press were molded into 25-mm discs (2 mm thick) for later use in rheological and thermal analysis. For mechanical testing, samples were pressed in the form of sheets, and "dogbones" were later punched out using a hydraulic press.

All rheological tests of the pure NBR and HNBR and their blend rubbers were carried out using a parallel-plate fixture with a diameter of 25 mm. The use of cone-and-plate geometry was not possible because of loading problems. For all samples, a strain amplitude of 15% was found to be in the linear viscoelastic range following strain sweep tests. The gap between parallel plates was fixed for all samples as 1.5 mm. The frequency, ω, sweep testing was carried out at 190°C in the range of ω = 0.01−100 rad/ s. All measurements were conducted using nitrogen as a convective heating medium to avoid any possible oxidation during the sweep tests. Reproducibility tests were performed for the 50/50 blend. Results are shown in *Fig. 1*. The agreement of both viscous and elastic properties shows the excellent reproducibility of the rheological measurements. In addition, frequency-temperature sweeps were performed in the range 200°C−230°C to obtain the flow activation energy of NBR, HNBR, and their blends. A thermal expansion coefficient of 2.5 microns/°C was used.

The thermal properties of the blends were measured calorimetrically at a heating rate of 5°C/min. A

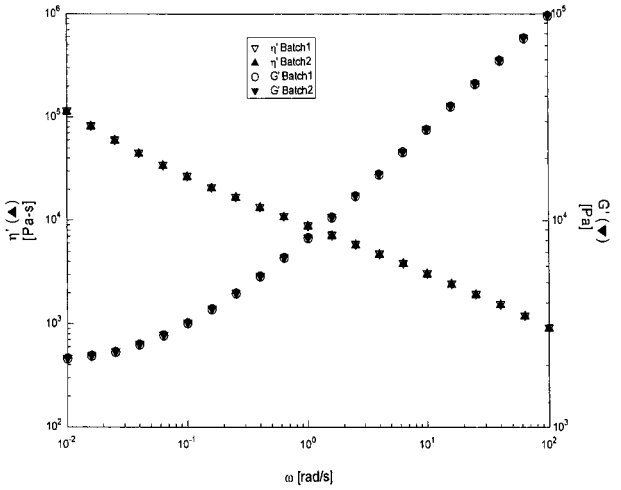

Fig. 1. Reproducibility test. η′(ω) and G′(ω) for 50/50 blend (T_{test} = 190°C, γ^o = 15%).

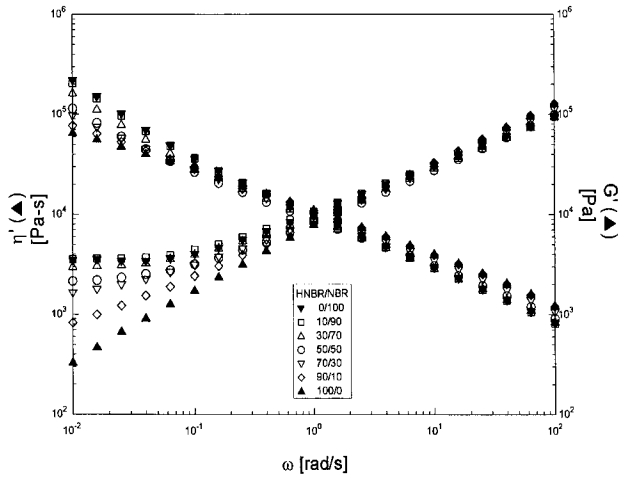

Fig. 2. η′(ω) and G′(ω) for blends, as well as the pure samples (T_{test} = 190°C, γ^o = 15%).

TA Instruments DSC 2910 equipped with Thermal Analyst 2200 software was used for this purpose. A blanket of nitrogen was maintained. Samples from the Carver press were used in this study. Samples of 5 to 10 mg were sliced and then compressed into aluminum pans for testing. Samples were cooled from room temperature to −80°C and then heated at 5°C/min 40°C. Thermal transitions were obtained from the heating cycle.

For the tensile properties, specimens were stamped out according to ASTM 638 (type V). The tensile tests were performed in an Instron 5567 tensile testing machine at room temperature. The gauge length was kept at 25 mm. The rate of grip separation was 520 mm/s (24). The results reported in this study were based on an average of a minimum of 5 samples.

A scanning electron microscope (JEOL-JSM-T-300) was used for the morphology studies. The objective was to get information regarding the size of the dispersed phase in to the matrix. A Jeol-Fine Coat Ion Sputter was used to coat a thin layer of gold on the specimen to avoid electrostatic charging during examination. The specimens were thereafter mounted on aluminum stubs for study.

RESULTS AND DISCUSSION

Rheological Analysis

Frequency sweep measurements were performed on blends of HNBR/NBR. Results for η′(ω) and G′(ω) for the 10%, 30%, 50%, 70%, and 90% HNBR blends and for the pure NBR and HNBR are shown in *Fig. 2*. At low-ω, η′(ω) data did not show a Newtonian plateau, suggesting a yield behavior. For all blends, values of η′ at all frequencies lie between the corresponding values of NBR and HNBR. The HNBR showed the lowest viscosity, and the increase in η′ of blends was proportional to the weight fraction of NBR. For G′(ω), results for the 10% HNBR blend were higher than the more elastic component (NBR) over a period of two decades. This positive deviation behavior (PDB) was also observed for other blend ratios. This behavior can easily be observed in *Fig. 3*, which shows a plot of tan δ (G″/G′) vs. ω. Also, the crossover modulus for HNBR-rich blends followed the linear rule of mixtures.

The increase in G′ for the 10%, 30%, 50%, and the 70% HNBR resulted in lower values of tan δ over almost two decades (0.01−1 rad/s). This low-ω range is sensitive to morphology. At high ω (>10 rad/s), values of tan δ were bounded between the pure components. However, such high frequencies are not used for the interpretation of miscibility data (20, 25, 26). The described behavior of η′ and G′ can easily be observed in plots of η′(ϕ) and G′(ϕ) given in *Figs. 4a* and *4b*, respectively. η′(ϕ) followed the log-additivity rule ($\eta'_{blend} = \sum \phi_i \log \eta_i$), while G′(ϕ) showed weak PDB. This is also evident in

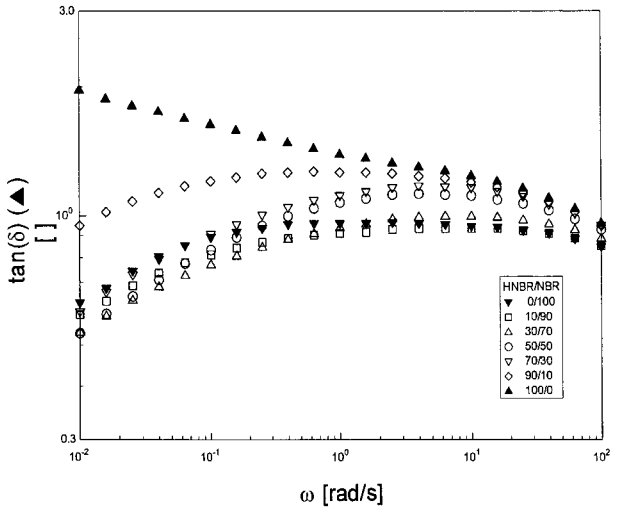

Fig. 3. Tan (δ) vs. ω for blends (T_{test} = 190°C, γ^o = 15%).

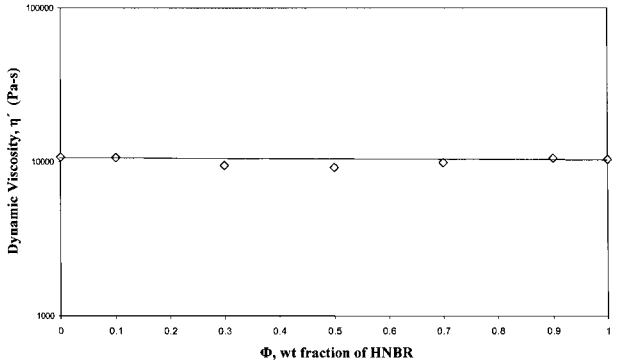

Fig. 4a. Dynamic viscosity η′(ϕ) as a function of weight fraction of HNBR. (ω = 0.03) (—) linear rule of mixture.

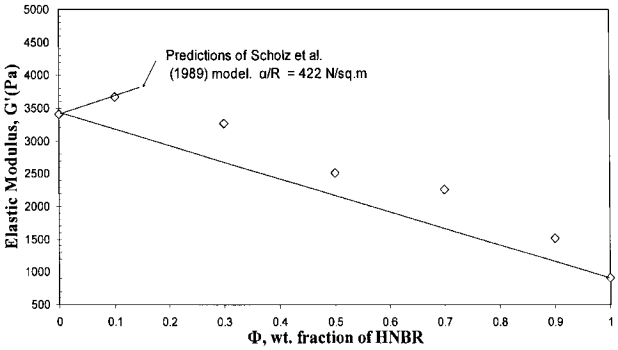

Fig. 4b. Elastic modulus G′(ϕ) as a function of weight fraction of HNBR (ω = 0.03) (—) linear rule of mixture.

the wide differences between the predictions of the dilute emulsion model of Scholz *et al.* (see *Fig. 4b*) and the experimental data. The estimated value of α/R, calculated from the model of Scholz *et al. (Eq 1)*, for the 10% and the 90% HNBR blends was 422 and 384 N/m^2, respectively. These values were in close agreement with previous reports of α/R for compatibilized blends (27). The small value of α/R is likely not a result of high droplet size since the viscosity data do not support this argument.

Hence, the experimental data of ω-sweep tests and model predictions suggest the presence of emulsion morphology of very small droplet size that did not have a significant influence on the viscosity. However, this emulsion morphology is suggested to have a very weak interface, as indicated by the small value of α/R. Hence, these blends are likely to be well dispersed at all compositions with very small droplet size. The suggested good dispersion is later validated by SEM micrographs.

In addition, the activation energy for the blends was calculated from the temperature-frequency sweep tests. The time-temperature superposition (TTS) principle was used to obtain master curves. The temperature was varied from 200°C to 230°C at a step of 10°C and the frequency range was 100 to 0.1 rad/s. A typical curve for the 50/50 blend is shown in *Fig. 5*. The flow

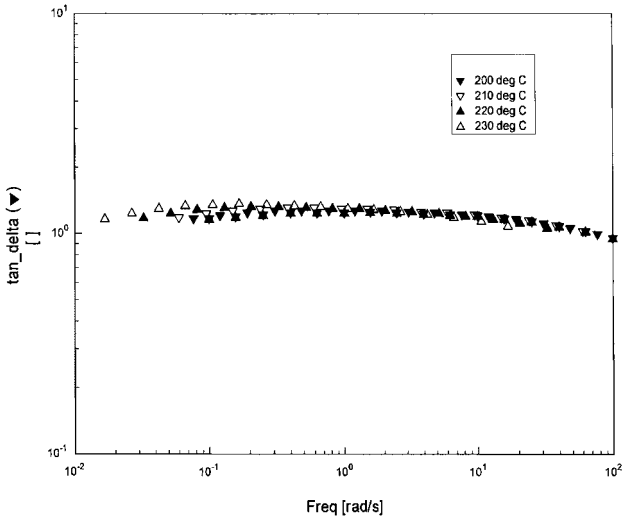

Fig. 5. Master curve for 90% HNBR blend. (T_{test} = 190°C, γ^o = 15%, T_{range} = 200°C−230°C).

activation energy, *E*, was calculated from the shift factor, a_T, using *Eq 2*:

$$\log a_T = \frac{E}{2.303R}\left(\frac{1}{T} - \frac{1}{T_o}\right) \tag{2}$$

where $a_T = \dfrac{\omega(T_o)}{\omega(T)}$; T and T_o are the current and reference temperature. The reference temperature was 210°C. Both a_T and *E* were calculated by ARES Orchestrator software.

The flow activation energies for NBR, HNBR, and their blends are displayed in *Fig. 6*. Values of E(ϕ) for HNBR/NBR blends approximately follow the inverse additivity rule $\left(1/E_b = \sum \dfrac{\phi_i}{E_i}\right)$.

Thermal Analysis

To investigate the compatibility of NBR/HNBR blends, DSC analysis was performed to measure T_g as a function of composition. Samples from the Carver

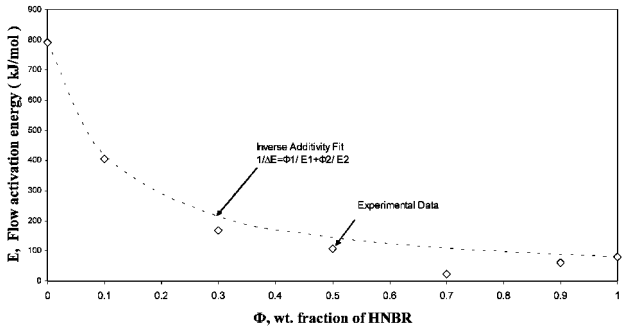

Fig. 6. Flow activation energy vs. weight fraction (ϕ) of HNBR.

press were analyzed according to the previously mentioned program. The glass transition for the more flexible HNBR was −25.32°C (T_{g1}), while that of the less flexible NBR was −13.36°C (T_{g2}). It is clear that all blends showed two glass transitions marked as T_{g1} and T_{g2}. Results of T_{g1} and T_{g2} for all blends are given in *Table 1*. From the table it can be seen that each brand of rubber has approximately retained its value of T_g in the blend and only slight variations were observed.

These results suggest the absence of segmental mixing; hence, the absence of a single T_g. The fact that the rheological measurements suggested the presence of small droplets supports these observations. It seems that the small droplet size suggested by the rheology was not small enough to produce segmental mixing of NBR and HNBR, which leads to a single T_g. Hence, these two blends are not thermodynamically miscible at the mixing temperature of 130°C. Yet, the blends could be mechanically compatible, as discussed in the following section.

Mechanical Analysis

Results of the mechanical testing are given in *Table 2*. The values of the displayed mechanical properties represent the average of at least 5 independent measurements, and the standard deviations show the range of these results. The tensile moduli as function of composition for blends of HNBR and NBR are shown in the table. The modulus for HNBR is 1.37 MPa, while that of the NBR is 1.61 MPa. The more flexible HNBR showed the least modulus and the unsaturated NBR was less flexible. In general, the moduli for the blends approximately follow the linear rule of mixtures. Similarly, the results for the stress at yield followed the linear rule of mixtures. These tabulated values suggest that at small deformations the blends show good compatibility.

At high strains, all blends as well as pure NBR and HNBR showed strain hardening. Tests were stopped because of slip, and we were not able to break any of the samples. Yet, a comparison of the stress at high strain (20 mm/mm) for all blends is given in *Table 2*. In this case, the HNBR (low modulus) showed a stress (2.25 MPa) that is higher than that of NBR (1.27 MPa). This suggests that HNBR undergoes a strain hardening at a rate higher than that of NBR. This strain hardening could be a result of induced crystallization, especially for this high ACN content HNBR (18). For the 10/90 or the 90/10 HNBR blends, the behavior of the stress at high strain is linear. However, around the 50/50 composition, the stress showed synergistic effects, which are likely due to the presence of a different morphology, as shown in the following section.

Table 1. T_g for NBR/HNBR Blends.

	5°C/min	
	T_{g1} (°C)	T_{g2} (°C)
NBR		−13.36
10%HNBR	−26.62	−13.23
30%HNBR	−25.71	−13.70
50%HNBR	−26.27	−14.20
70%HNBR	−25.93	−12.82
90%HNBR	−26.01	−14.49
HNBR	−25.32	

SEM

The SEM surface micrographs for the 10/90; 50/50; and 90/10 HNBR/NBR blends are shown in *Figs. 7a, b,* and *c*, respectively. The 10/90 HNBR/NBR blend (*Fig. 7a*) shows a dispersed and somewhat uniform morphology. The observed small clusters could be a result of the less flexible nature of the NBR, which might have inhibited the dispersion of HNBR. These clusters could explain the increase in G′, which resulted in tan δ values that are lower than that of the more elastic component (NBR), as shown in *Fig. 3*. On the other hand, the 90/10 HNBR/NBR blend (*Fig. 7c*) shows a uniform, emulsion-like morphology, which could be attributed to the flexible nature of the HNBR matrix. This observation is supported by the previous rheological measurements shown in *Fig. 3*. There, the value of tan δ for the 90/10 HNBR blend was bounded by the corresponding values of NBR and HNBR. From *Figs. 7a* and *7c* it is clear that the 90/10 HNBR/NBR blend (*Fig. 7c*) is closer to emulsion morphology than the 10/90 HNBR/NBR blend. For the 50/50 HNBR/NBR blend, the SEM micrograph suggests a co-continuous morphology, where both phases are continuous, rather than emulsion morphology. This could be due to insufficient shear stress for disrupting these structures. Similar morphology was reported for blends of NBR and natural rubber (6).

Table 2. Results of the Mechanical Analysis of NBR/HNBR Blends.

Wt Fraction of HNBR	Modulus (MPa)	Std Dev	Stress at Yield (MPa)	Std Dev	Stress at High Strains (MPa)	Std Dev
0	1.60798	0.143589	0.862843	0.090107	0.862843	0.118346
0.1	1.588	0.136207	0.88552	0.071352	0.88552	0.166179
0.3	1.39396	0.079777	0.855558	0.051169	0.855558	0.078898
0.5	1.471429	0.149268	0.91865	0.056594	0.91865	0.133195
0.7	1.368	0.134091	0.679167	0.052556	0.679167	0.224368
0.9	1.4004	0.117119	0.6733	0.041706	0.6733	0.16268
1	1.366813	0.081013	0.732622	0.036079	0.732622	0.141514

Fig. 7a. SEM micrographs for 10/90 HNBR/NBR blends.

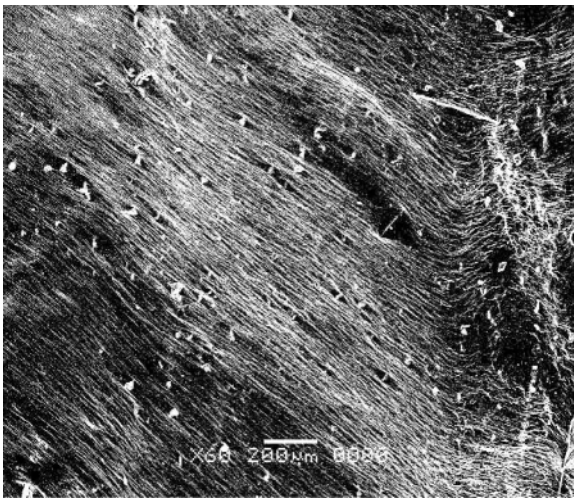

Fig. 7b. SEM micrographs for 50/50 HNBR/NBR blends.

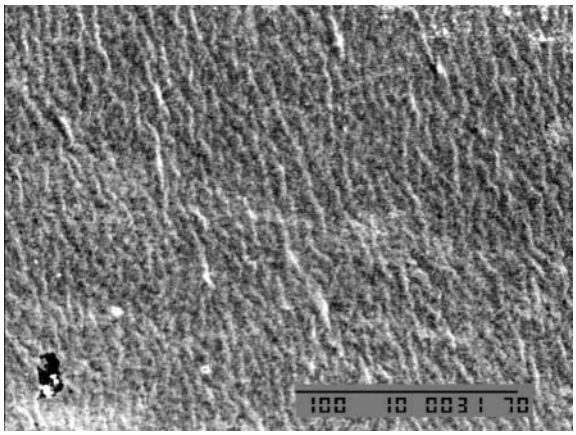

Fig. 7c. SEM micrographs for 90/10 HNBR/NBR blends.

CONCLUSION

In this study, HNBR and NBR of very similar acrylonitrile content and Mooney viscosity were blended at different compositions. The blends of the more flexible HNBR and the less flexible unsaturated NBR show interesting rheological, thermal, and mechanical properties. The dynamic viscosity of the blends followed the log-additivity rule, while the flow activation energy closely followed inverse additivity rule. On the other hand, the storage modulus showed synergistic effects at all compositions, suggesting the presence of weak emulsion morphology at both ends of the composition range. This conclusion is supported by thermal analysis that showed the presence of two glass transitions, representing the pure components, at all blend ratios. For the 50/50 HNBR/NBR blend, the SEM micrographs suggest a co-continuous morphology. The small strain mechanical properties such as tensile modulus and yield stress followed linear additivity. However, HNBR was observed to strain harden at a rate higher than that of NBR. Induced crystallization of HNBR was suggested as a reason for the strain hardening of HNBR-rich blends. In conclusion, the different rheological, thermal, and mechanical testing techniques agree in suggesting that the structurally similar HNBR and NBR are not thermodynamically miscible but mechanically compatible.

ACKNOWLEDGMENTS

The authors thank KFUPM for its support for this research. Zeon Chemicals, USA, is acknowledged for providing the samples. We also thank Professor Michael C. Williams and Dr. Jiang Bai of the University of Alberta, Canada, for their help with the DSC analysis. Mr. Abdul Aleem of the Mechanical Engineering Department, KFUPM, is acknowledged for his help with the SEM scans.

REFERENCES

1. W. Hofmann, *Rubber Chem Technol.*, **37**, 52 (1963).
2. D. N. Schulz, S. R. Turner, and M. A. Golub, *Rubber Chem Technol.*, **55**, 809 (1982).
3. S. Bhattacharjee, A. K. Bhowmick, and B. Avasthi, *Modification of Properties of Nitrile, Handbook of Engineering Polymeric Materials*, N. P. Cheremisinoff, ed., Dekker, New York (1997).
4. A. N. Da Silva, M. Rocha, F. M. Coutinho, R. Bretas, and M. Farah, *Polymer Testing*, **21**, 647 (2002).
5. S-H. Zhu and C-M. Chan, *Polym. Eng. Sci.*, **39**, 1998 (1999).
6. C. Sirisinha, S. Limcharoen, and J. Thunyarittikorn, *J. Appl. Polym. Sci.*, **85**, 1232 (2001).
7. M. J. K. Chee, J. Ismail, C. Kummerlowe, and H. Kammer, *Polymer*, **43**, 1235 (2002).
8. S. Saha, *Eur. Polym. J.*, **37**, 399 (2001).
9. S. Saha, *Eur. Polym. J.*, **37**, 2513 (2001).
10. C. Boisserie and R. H. Marchessault, *J. Polym. Sci.*, **15**, 1211 (1977).
11. D. K. Setua, C. Soman, A. K. Bhowmick and G. N. Mathur, *Polym. Eng. Sci.*, **42**, 10 (2002).
12. J. H. Lee, J. K. Lee, K. H. Lee and C. H. Lee, *Polymer Journal*, **32**, 321 (2000).
13. A. Y. Coran, R. Patel and D. Williams, *Rubber Chem. Technol.*, **58**, 1014 (1985).

14. P. Anthony and S. K. De, *Rubber Chem. Technol.*, **7**, 376 (1997).
15. J. Clarke, B. Clarke and P. K. Freakley, *Rubber Chem Technol*, **74**, 1 (2000).
16. S. J. Ahn, K. H. Lee, B. K. Kim and H. M. Jeong, *Appl. Polym. Sci.*, **78**, 1861 (2000).
17. O. Chung and A. Y. Coran, *Rubber Chem Technol.*, **70**, 781 (1987).
18. G. Severe and J. White, *J. Appl. Polym. Sci.*, **78**, 1521 (2000).
19. A. Jha and A. K. Bhowmick, *Rubber Chem. Technol.*, **70**, 798 (1997).
20. P. Scholz, D. Froelich, and R. Muller, *J. Rheol.*, **33**, 481 (1989).
21. D. R. Paul, *Polymer Blends*, 2nd Ed., Academic Press, New York (2001).
22. L. A. Utracki, *Polymer Alloys and Blends: Thermodynamics and Rheology*, Hanser, New York (1989).
23. R. A. Chaudhry, "Degradation of NBR and HNBR: Rheological, light scattering and Molecular Simulation Study," *MS Thesis*, KFUPM, Dhahran (January 2004).
24. R. P. Brown, Physical Testing of Rubber, 2nd Ed., Elsevier Applied Science Publishers, New York (1986).
25. T. Hameed and I.A. Hussein, *Polymer*, **43**, 6911 (2002).
26. I. A. Hussein, *Macromolecules*, **36**, 2024 (2003).
27. B. Brahimi, A. Ait-Kadi, A. Ajji, R. Jerome and R. Fayt, *J. Rheol.*, **35**, 1069 (1991).